Image Compression by Spline Wavelets Orthogonal with Respect to Weighted Sobolev Inner Product

Hiroki Sugiyama and Masaru Kamada
Department of Computer and Information Sciences
Ibaraki University, Hitachi, 316-8511 Japan
kamada@mx.ibaraki.ac.jp

Rensten Enkhbat
Department of Mathematics and Computer
National University of Mongolia, Ulaanbaatar, Mongolia
renkhbat46@ses.edu.mn

Abstract

Application of Sobolev spline wavelets to image compression is reported. The wavelets are constructed to be orthogonal with respect to the weighted Sobolev inner product which is defined by a weighted sum of the integrated product of two functions and that of their derivatives. It is shown that a larger weight on the latter decreases contouring artifacts in smooth portions of compressed images at the expense of decreased overall sharpness.

1 Introduction

Discrete wavelet transform is a standard technique for lossy image compression. Most of the wavelets have been created so that they are orthogonal with respect to the standard inner product

$$\langle f, g \rangle_{L^2} = \int_{-\infty}^{\infty} f(t)\overline{g(t)}dt \tag{1}$$

in $L^2(R)$. Compressed images by means of those wavelets are the best approximation of the original images in the sense that the mean square error in brightness is minimized for a limited number of coefficients.

It has been widely known that the human vision is sensitive to spatial changes in brightness [Morgan, 2005]. So we might obtain a better image compression algorithm by caring about the mean square error in spatial changes as well as absolute values of brightness.

Sobolev space $H^1(R)$ that has a weighted Sobolev inner product

$$\langle f, g \rangle_{H^1} = \int_{-\infty}^{\infty} f(t)\overline{g(t)} + \rho^2 f'(t)\overline{g'(t)}dt \tag{2}$$

with the weight $\rho > 0$ is a Hilbert space where we can construct a multiresolution analysis in terms of wavelets. Among results of the mathematical literature on wavelets for the general Sobolev spaces, there are integral wavelet transform [Chuong and Tri, 2002], compactly supported orthogonal wavelets [Bastin and Laubin, 1997], orthogonal wavelets for the space of box splines [He and Lai, 1988], and semi-orthogonal cubic spline wavelets [Wang, 1996]. Those wavelets seem promising better image compression algorithms but have never been applied to real images.

This paper presents an experimental study of image compression by a wavelet which is orthogonal with respect to the weighted Sobolev inner product. The signal space is limited to those consisting of cardinal polynomial splines including the cubic ones that have been popular in image representation [Unser, Aldroubi and Eden, 1991]. We first construct a semi-orthogonal wavelet so that it is orthogonal to shifted B-spline scaling functions with respect to the weighted Sobolev inner product. Then, by orthogonalizing the shifted scaling functions and the shifted semi-orthogonal wavelets individually, we obtain a pair of orthogonal scaling function and wavelet of which shifts are mutually orthogonal. Finally they are applied to image compression where wavelet coefficients having less magnitude are discarded.

Experiments with a few test images and various weight ρ show that the Sobolev-orthogonal spline wavelet with a certain $\rho > 0$ provides more natural looking images at smooth portions where the standard wavelet with $\rho = 0$ produces contouring artifacts. In exchange of this effect, the whole image looks out of focus as we set a larger blending parameter ρ. A good compromise for the test images is found to be around $\rho = 0.2$.

2 B-spline and compactly supported semi-orthogonal wavelet

We start from the B-spline scaling function of order m defined by

$$\varphi_m(x) = \frac{1}{(m-1)!}\sum_{k=0}^{m}(-1)^k\binom{m}{k}(x-k)_+^{m-1}, \tag{3}$$

where

$$(x-k)_+^{m-1} = \begin{cases} (x-k)^{m-1}, & x > k \\ 0, & \text{otherwise,} \end{cases}$$

which satisfies the two-scale relation

$$\varphi_m(x) = \sum_k p_k \varphi_m(2x-k), \tag{4}$$

where

$$p_k = \begin{cases} \frac{1}{2^{m-1}}\binom{m}{k}, & k = 0, 1, \cdots, m \\ 0, & \text{otherwise.} \end{cases} \tag{5}$$

A wavelet associated with this scaling function must be expressed in the form

$$\psi_m(x) = \sum_k q_k \varphi_m(2x-k) \tag{6}$$

and must satisfy

$$\langle \varphi_m(\cdot), \psi_m(\cdot - n) \rangle_{H^1} = 0. \tag{7}$$

Mimicking the method [Chui and Wang, 1992] of deriving compactly supported wavelets with respect to the standard inner product $\langle \cdot, \cdot \rangle_{L^2}$, we find a set of two-scale coefficients q_k that satisfy (7) as follows:

$$q_k = \begin{cases} \dfrac{(-1)^k}{2^{m-1}} \displaystyle\sum_{l=0}^{m} \binom{m}{l} \Big\{ \varphi_{2m}(k-l+1) \\ \qquad +\rho^2 \big(2\varphi_{2m-2}(k-l) \\ \qquad\qquad -\varphi_{2m-2}(k-l-1) \\ \qquad\qquad -\varphi_{2m-2}(k-l+1)\big) \Big\}, \\ \qquad\qquad k=0,1,\cdots,3m-2 \\ 0, \ \text{otherwise.} \end{cases} \tag{8}$$

This ψ_m is a semi-orthogonal wavelet of which shifts are not orthogonal to one another.

3 Orthogonal scaling functions and orthogonal wavelets

For the purpose of data compression, the scaling function and wavelet had better be orthogonal to their shifts, respectively. By following the general method [Aldroubi, Unser and Eden, 1992] of orthogonalizing a shift-invariant basis, we transform φ_m and ψ_m into their orthogonal versions $\widetilde{\varphi}_m$ and $\widetilde{\psi}_m$, respectively, as follows.

An orthogonal scaling function $\widetilde{\varphi}_m$ must be expressed in the form

$$\widetilde{\varphi}_m(x) = \sum_k \alpha_k \varphi_m(x-k) \tag{9}$$

and must satisfy

$$\langle \widetilde{\varphi}_m(\cdot), \widetilde{\varphi}_m(\cdot - n) \rangle_{H^1} = \begin{cases} 1, & n=0 \\ 0, & n \neq 0. \end{cases} \tag{10}$$

A set of coefficients α_k that makes (10) hold good is given by

$$\alpha_k = \frac{1}{2\pi} \int_0^{2\pi} \frac{e^{-i\omega k}}{\left(\sum_l \big\{ \varphi_{2m}(m-l) + \rho^2 \big(2\varphi_{2m-2}(m-l) - \varphi_{2m-2}(m-l-1) - \varphi_{2m-2}(m-l+1)\big) \big\} e^{-i\omega l} \right)^{\frac{1}{2}}} d\omega. \tag{11}$$

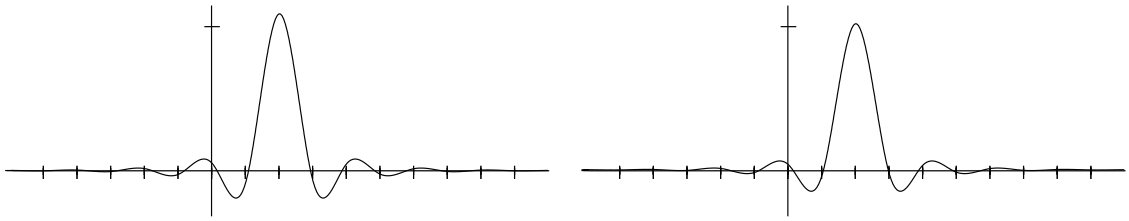

(a) $\widetilde{\varphi}_m$ $(\rho = 0)$ (b) $\widetilde{\varphi}_m$ $(\rho = 0.2)$

Figure 1: Orthogonal scaling functionsi$m = 4$j

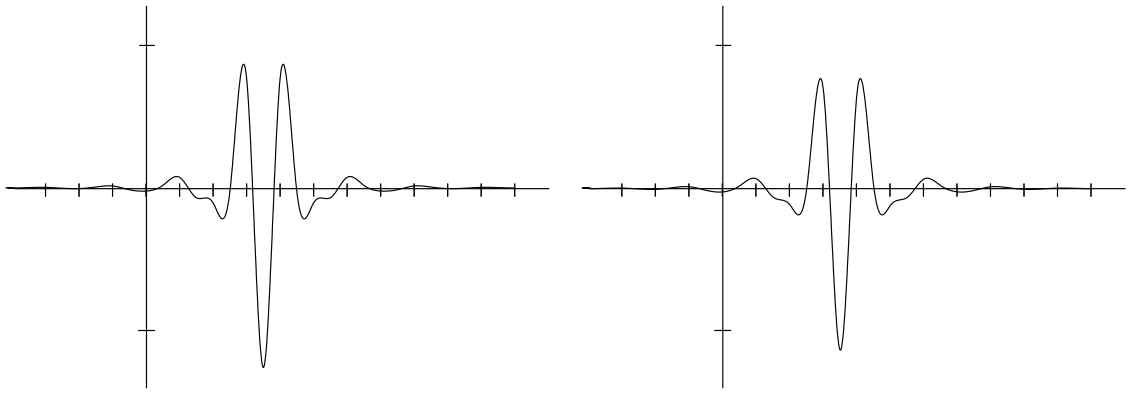

(a) $\widetilde{\psi}_m$ $(\rho = 0)$ (b) $\widetilde{\psi}_m$ $(\rho = 0.2)$

Figure 2: Orthogonal waveletsi$m = 4$j

An orthogonal wavelet $\widetilde{\psi}_m$ must also be expressed in the form

$$\widetilde{\psi}_m(x) = \sum_k \beta_k \psi_m(x-k) \tag{12}$$

and must satisfy

$$\langle \widetilde{\psi}_m(\cdot), \widetilde{\psi}_m(\cdot - n) \rangle_{H^1} = \begin{cases} 1, & n = 0 \\ 0, & n \neq 0. \end{cases} \tag{13}$$

A set of coefficients β_k that makes (13) hold good is given by

$$\beta_k = \frac{1}{2\pi} \int_0^{2\pi} \frac{e^{-i\omega k}}{\left(\begin{array}{l} \sum_n \sum_a \sum_b \frac{1}{2} q_a q_b \Big(\varphi_{2m}(m+2n-a+b) \\ \qquad + \rho^2 \big(2\varphi_{2m-2}(m+2n-a+b-1) \\ \qquad\quad - \varphi_{2m-2}(m+2n-a+b) \\ \qquad\quad - \varphi_{2m-2}(m+2n-a+b-2) \big) \Big) e^{-i\omega n} \end{array} \right)^{\frac{1}{2}}} d\omega. \tag{14}$$

Examples of $\widetilde{\varphi}_m$ and $\widetilde{\psi}_m$ are plotted in Figs. 1 and 2, respectively in the cubic spline case ($m = 4$). Their overall shapes look almost the same irrespective to the weight ρ. A close look at them reveals subtle but interesting differences. The scaling function in the case

$\rho = 0.2$ has a wider and less tall main peak and less oscillating tails in Fig. 1(b) compared to the case of $\rho = 0$ in Fig. 1(a) . The wavelet in the case $\rho = 0.2$ has less tall but quicker central oscillations in Fig. 2(b) compared to the case of $\rho = 0$ in Fig. 2(a) . This suggests that a larger weight ρ makes the scaling function and the wavelet less and more sharp, respectively, around their central positions.

With a help of the inversion formula

$$\varphi_m(x) = \sum_k \alpha_k^* \widetilde{\varphi}_m(x-k) \tag{15}$$

of (9), where

$$\alpha_k^* = \frac{1}{2\pi}\int_0^{2\pi} \left(\begin{array}{l} \sum_l \Big\{ \varphi_{2m}(m-l) \\ \qquad +\rho^2 \big(2\varphi_{2m-2}(m-l) \\ \qquad\qquad -\varphi_{2m-2}(m-l-1) \\ \qquad\qquad -\varphi_{2m-2}(m-l+1) \big) \Big\} e^{-i\omega l} \end{array} \right)^{\frac{1}{2}} e^{-i\omega k} d\omega, \tag{16}$$

we can calculate the two-scale coefficients

$$\widetilde{p}_k = \sum_l \sum_n \alpha_l \alpha_n^* p_{k-2l-n} \tag{17}$$

$$\widetilde{q}_k = \sum_l \sum_n \beta_l \alpha_n^* q_{k-2l-n} \tag{18}$$

that fit the two-scale relations

$$\widetilde{\varphi}_m(x) = \sum_k \widetilde{p}_k \widetilde{\varphi}_m(2x-k) \tag{19}$$

$$\widetilde{\psi}_m(x) = \sum_k \widetilde{q}_k \widetilde{\varphi}_m(2x-k) \tag{20}$$

for the orthogonal scaling function and wavelet.

Sampled values s_l and coefficients $\widetilde{c}_k^{(0)}$ are related by

$$s_l = \sum_k \widetilde{c}_l^{(0)} \widetilde{\varphi}_m(l-k). \tag{21}$$

and

$$\widetilde{c}_k^{(0)} = \sum_l b_{k-l} s_l, \tag{22}$$

where

$$b_k = \frac{1}{2\pi}\int_0^{2\pi} \frac{e^{i\omega k}}{\sum_l \widetilde{\varphi}_m(k-l) e^{-i\omega l}} d\omega. \tag{23}$$

(a) lena (b) pepper

Figure 3: Original test images

The wavelet decomposition and reconstruction are performed by the recurrence formulae

$$\widetilde{c}_l^{(j+1)} = \sum_k \widetilde{p}_{k-2l}\widetilde{c}_k^{(j)}, \qquad \widetilde{d}_l^{(j+1)} = \sum_k \widetilde{q}_{k-2l}\widetilde{c}_k^{(j)} \tag{24}$$

and

$$\widetilde{c}_l^{(j)} = \sum_k \left\{ \widetilde{p}_{l-2k}\widetilde{c}_k^{(j+1)} + \widetilde{q}_{l-2k}\widetilde{d}_k^{(j+1)} \right\}, \tag{25}$$

respectively.

4 Experiment

Test images of Fig. 3 have the resolution of 512×512 pixels. The wavelet decomposition was performed on an image for three times in each of horizontal and vertical directions. Then we obtained 64×64 scaling coefficients that represent a shrunken version and wavelet coefficients that represent details. From the coefficients, a compressed image was reconstructed without wavelet coefficients having less magnitude.

Figures 4–9 show the compressed images by cubic splines ($m = 4$) with different discarding ratios and the weights $\rho = 0$, 0.1, 0.2, and 0.3. In Figs. 4 and 5 where we discarded the 99% wavelet coefficients, the Sobolev-orthogonal wavelet with $\rho > 0$ provides more natural looking images at smooth portions where the standard wavelet with $\rho = 0$ produces contouring artifacts. In exchange of this effect, the whole image looks rather out of focus as we set larger ρ. A good compromise for the test images seems to be around $\rho = 0.2$. The above observation is less evident but still true of Figs. 6–7 and Figs. 8–9 where we discarded 95% and 90% of the wavelet coefficients, respectively.

(a) $\rho = 0$ (b) $\rho = 0.1$

(c) $\rho = 0.2$ (d) $\rho = 0.3$

Figure 4: lena with 99% of wavelet coefficients discarded

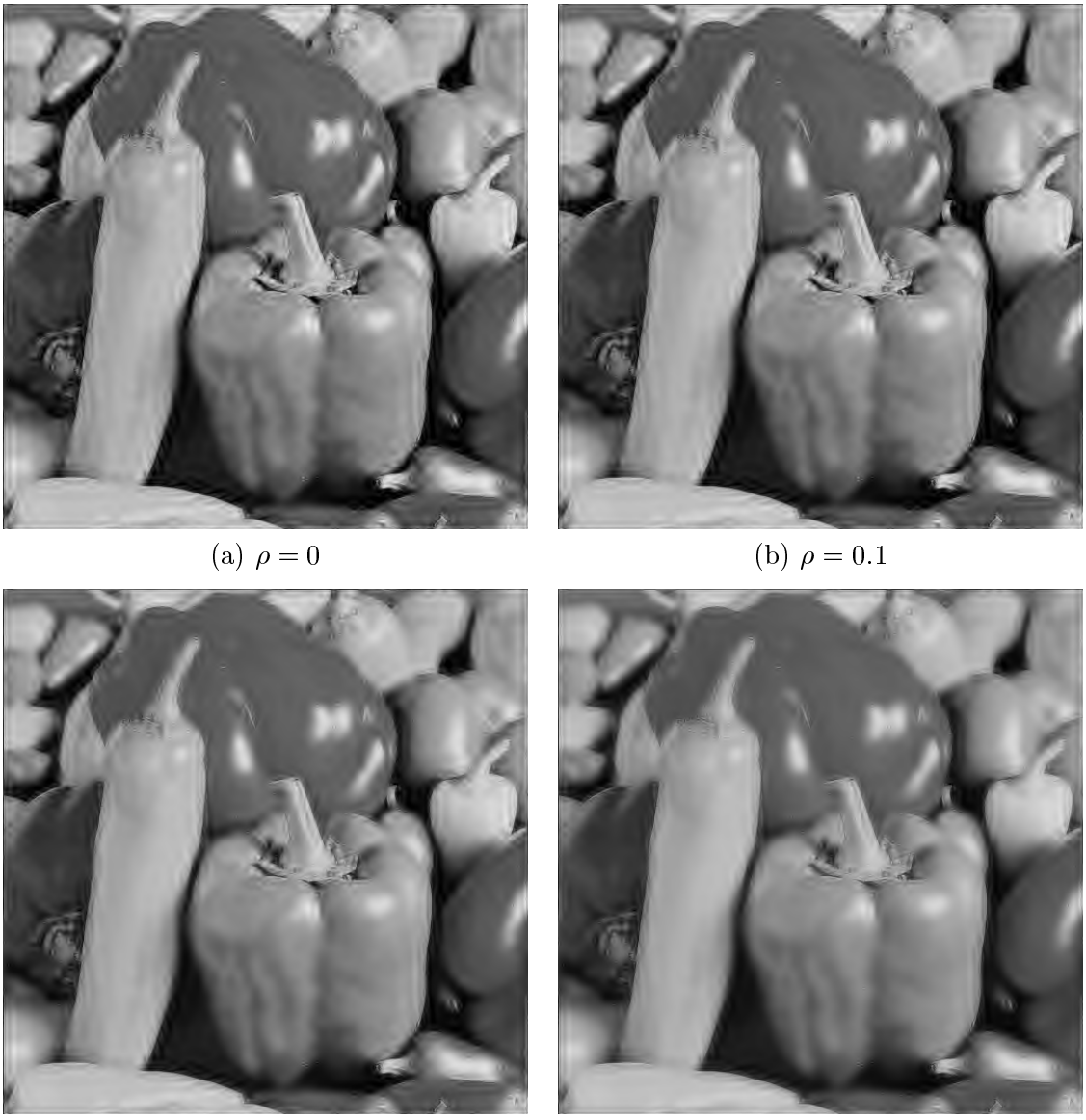

(a) $\rho = 0$ (b) $\rho = 0.1$

(c) $\rho = 0.2$ (d) $\rho = 0.3$

Figure 5: pepper with 99% of wavelet coefficients discarded

(a) $\rho = 0$ (b) $\rho = 0.1$

(c) $\rho = 0.2$ (d) $\rho = 0.3$

Figure 6: lena with 95% of wavelet coefficients discarded

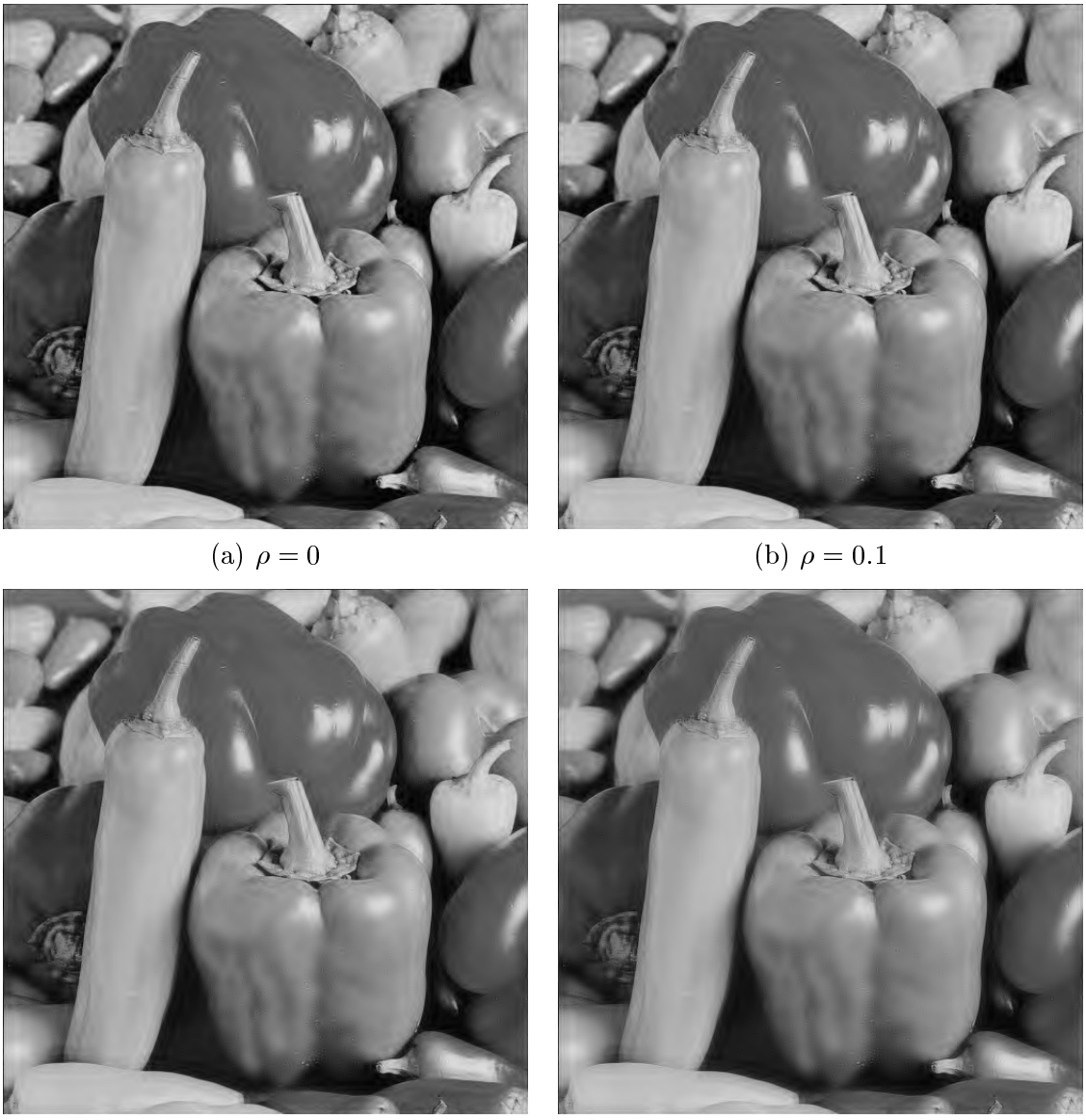

(a) $\rho = 0$ (b) $\rho = 0.1$

(c) $\rho = 0.2$ (d) $\rho = 0.3$

Figure 7: pepper with 95% of wavelet coefficients discarded

(a) $\rho = 0$ (b) $\rho = 0.1$

(c) $\rho = 0.2$ (d) $\rho = 0.3$

Figure 8: lena with 90% of wavelet coefficients discarded

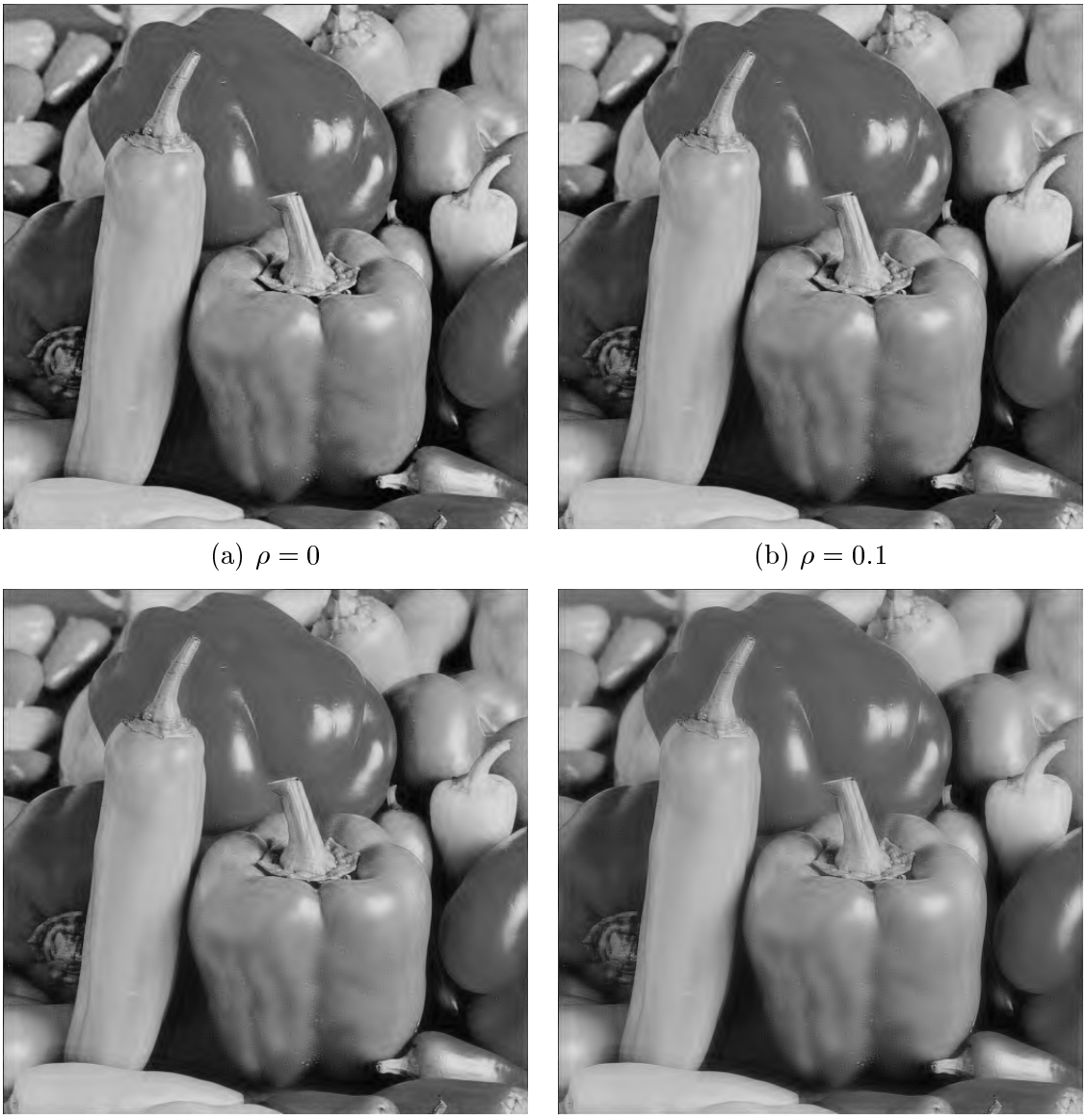

(a) $\rho = 0$ (b) $\rho = 0.1$

(c) $\rho = 0.2$ (d) $\rho = 0.3$

Figure 9: pepper with 90% of wavelet coefficients discarded

5 Conclusions

Orthogonal spline wavelets in the sense of the weighted Sobolev inner product were applied to image compression. It has been shown that a larger weight ρ decreases contouring artifacts in smooth portions of compressed images at the expense of decreased overall sharpness. So we may use the weight as a parameter to control the "anti-aliasing" effect in image representation.

Similar experiments should be done in the future by employing other Sobolev kind of wavelets such as those presented in [Bastin and Laubin, 1997] and [He and Lai, 1988].

References

A. Aldroubi, A., Unser, M. and Eden, M., (1992) Cardinal spline filters: Stability and convergence to the ideal sinc interpolator. *Signal Processing*, vol.28, nr.2, pp.127–138.

Bastin, F., and Laubin, P., (1997) Regular compactly supported wavelets in Sobolev spaces. *Duke Math. J.*, vol.87, nr.3, pp.481–508.

Chui, C. K., and Wang, J. Z., (1992) On compactly supported spline wavelets and a duality principle. *Trans. Amer. Math. Soc.*, vol.330, pp.903–915.

Chuong, N. M., and Tri, T. N., (2002) The integral wavelet transform in weighted Sobolev spaces. *Abstract and Applied Analysis*, vol.7, pp.135–142.

He, W., and Lai, M.-J., (1988) Bivariate box spline wavelets in Sobolev spaces. *Proc. SPIE*, vol.3458, Wavelet Applications in Signal and Imaging Processing VI, pp.56–66.

Morgan, M., (2005) *The Space Between Our Ears: How the Brain Represents Visual Space*, Oxford University Press, New York.

Unser, M., Aldroubi, A., and Eden, M., (1991) Fast B-spline transforms for continuous image representation and interpolation. *IEEE Trans. Pattern Anal. Machine Intelli.*, vol.13, nr.3, pp.277–285.

Wang, J., (1996) Cubic spline wavelet bases of Sobolev spaces and multilevel interpolation. *Appl. Comput. Harmonic Analysis*, vol.3, nr.2, pp.154–163.